Low-Cost PFC Analyzer for Early Anode Effect Detection

Hervé Roustan
R&D Process Control Team Leader
Rio Tinto Aluminium Pechiney, Saint Jean de Maurienne, France
Corresponding author: herve.roustan@riotinto.com

Abstract

The anode effect is a major and unfortunately recurrent malfunction of aluminum reduction cells. Process control algorithms implemented in the pot controller can detect this problem and eliminate it. However, detection is based on the resulting significant increase in the voltage of the pot, and this increase is generally very fast: the nominal voltage is increased to 8 Volts (the detection threshold commonly used by ALPSYS®, for AP technology pots) in just a few seconds, which is not enough to permit a preventive treatment of the anode effect.

However, several minutes before the anode effect can be detected with certainty by a rise in the pot voltage, the unwanted electrochemical reaction is already present and gases such as CF_4 or C_2F_6 are already being produced by the pot. This phenomenon has been clearly demonstrated on prototype pots equipped with Fourier transform infrared analyzers (FTIR). Unfortunately, such analyzers cost too much to allow equipping all the pots in a smelter with them. We have therefore worked in partnership with the Mirsense company to develop a low-cost device for continuously sampling and analyzing pot gases in order to detect CF_4. The principle of the device is photo-acoustic detection: a laser emitting at a carefully chosen frequency will selectively excite CF_4 molecules so that they emit a sound whose amplitude is directly related to the quantity of CF_4 present. The development of this device also includes the sampling equipment, in order to obtain a solution able to work continuously over a long time without manual intervention.

To date, the performance of our photo-acoustic device is very good and its results consistent with those of an FTIR placed in parallel for comparison.

Keywords: Anode effect, PFC. Low-cost PFC analyser.

1. Introduction

The anode effect is a phenomenon which appears in aluminum reduction cells due to the depletion of oxygen-containing ions at the anode. It is generally considered that the effect occurs when the alumina concentration in the pot is less than 1 to 1.5 % wt. [1], [2], [3], [4], [5]. At the beginning of the aluminum industrial era, there was no automated alumina feed, and the anode effect was awaited in order to know when to add more alumina to the pot. For several decades now, thanks to automation, the pots have been equipped with either continuous or semi-continuous alumina feeding systems. The appearance of anode effects is therefore no longer necessary to ensure the proper functioning of the pots and is clearly not desirable, because the phenomenon has negative consequences on the robustness of pots (release of intense thermal energy which deteriorates ledge and crust) and on their performance (higher energy consumption and lower current efficiency). Moreover, the anode effect causes a release of CF_4 and C_2F_6 instead of the CO_2 normally produced at the active surface of the anodes. These two perfluorocarbons (PFCs) have a global warming potential of respectively about 7 000 to 12 000 times that of CO_2 and have an extremely long lifetime in the atmosphere, reaching respectively 50 000 and 10 000 years. This is why it is important to limit the occurrence of anode effects as much as possible (expressed in number of anode effects per pot and per day). Much progress has been made in this field since the 1990s, in particular by trying to improve the operating conditions of the pots.

Numerous scientific studies have been carried out to explain the origins of anode effects [6], [7], [8], [9]. All these studies clearly show that the primary cause of the anode effect is the lack of alumina in the pot or more precisely under certain anodes. It seems that since alumina is delivered at the center of the pot, an anode effect is very often triggered under the anodes at the end of the pot, in areas where the bath stirring is less powerful and where enriching the bath with alumina is therefore more difficult. As soon as the alumina concentration under these anodes drops below approximately 1 to 1.5 % wt., the anodic current density limit is reached and the first bubbles of CF_4 and C_2F_6 begin to form [4], creating a resistive layer under these anodes which further reduces their current. This current reduction is distributed to the other anodes, increasing their current densities and hence making them more sensitive to the anode effect. A chain reaction then occurs, generalizing the anode effect to all the anodes of the pot [3].

However, as the first anodes undergo the anode effect, the new current distribution in the other anodes is not clearly visible in the pot voltage, because other phenomena such as magnetic instability lead to noise in the voltage greater than the variations resulting from the onset of the anode effect on the first anodes [10]. For this reason, the anode effect is only clearly detectable in the very last seconds before it generalizes, when the cell voltage begins to increase rapidly.

Thus, the initiation of the anode effect results in a drastic drop in current density in a limited number of anodes. Studies have therefore been carried out to detect the phenomenon by monitoring the current in each anode [11] [12]. This method is very effective but requires equipping each pot with anode current sensors, which is quite costly.

Other authors have used statistical methods, in particular principal component analysis [12] [13], or the calculation of third-order coherence functions [14] in order to detect drifts in the process and in particular in alumina depletion. However, the monitoring of these indicators is not sufficient because many exogenous phenomena can intervene. For example, monitoring the number of alumina shots introduced into the pot per unit of time is a good indicator of the quantity present in the pot, but a significant reduction in this value will not necessarily mean a reduction in the concentration, as this may be caused by a collapse of the cover in the bath (the regulation algorithm then decreases the alumina shot frequency to take account of this parasitic alumina feeding). It is also possible to estimate the alumina concentration in the pot using a linear Kalman filter, in order to increase the feeding rate (i.e., overfeeding) in case of lack of alumina [15], [16]. However, these estimators need to be readjusted periodically.

Studies using machine learning techniques have also already been used in order to predict the anode effect [17]. We can cite the work of Meghlaoui et al. in 1998 [18]. These authors used neural networks for the prediction of cell resistance at the 15-minute horizon. Their one-layer neural network uses as input data the instantaneous resistance value and its value 5, 10 and 15 minutes before, the instantaneous alumina feed rate and that, 20 minutes before, as well as the slope of the resistance and its deviation from the minimum recorded value. It should be noted that the authors claim good results in reducing anode effects thanks to their algorithm which imposes alumina overfeeding as soon as the prediction foresees an increase in resistance above a critical threshold. Nevertheless, this algorithm is open to criticism because, although the numerous overfeeds avoid the anode effects, their high frequency leads to an excess of alumina in the pots causing sludge. This algorithm has never been put into production on an industrial scale. More recently, Zhou et al. [19] used a generalized regression neural network. They also used aggregated input data (13 in total) such as average voltage for the last 3 hours, average voltage for the last 8 hours, average alumina feed rate for the last 24 hours, etc. As output, the model predicts a probability of occurrence of an anode effect in the next 30 minutes. Once again, the number of false positives seems too high to consider applying this method to all the pots in a plant.

Finally, work has been carried out that focused on signal processing algorithms and, more specifically, on wavelet transforms [20] [21]. Zhang [21] notably proposes to transform the resistance signal into 4 layers of 8th order Daubechies wavelets. This allows it to distinguish the resistance in the 30 minutes preceding an anode effect from that when the pot is operating correctly.

Other methods for predicting an approaching anode effect (like rate of voltage rise, hysteresis in the voltammogram curve, measuring acoustic or high frequency electrical noise, etc.) have also been investigated (see Haupin et al. [22]) To date, these methods do not seem to have been used in industrial pot control algorithms, maybe due to a high rate of false positives.

Another possibility for predicting anode effects is to continuously measure CF_4 concentration in pot gases. Indeed, as described previously, the beginning of an anode effect is characterized by the reaching of the current limit under a first anode, producing CF_4 and C_2F_6 without any visible effect on the pot voltage. The detection of these first "bubbles" of CF_4 is therefore clearly a harbinger of an anode effect.

Continuous pot gas analysis devices are already existing. They are based on technologies such as Fourier Transform Infra-Red spectroscopy (FTIR) or use Quantum Cascade Laser (QCL) [23]. These devices are very sensitive and have made it possible to demonstrate that a non-negligible part of the PFCs emitted by the cell occurs before the anode effect is declared (when the voltage of the pot exceeds a threshold - generally about 8 volts) that is as soon as the depletion of oxyfluoride ions under an anode leads to the current limit being reached [24], [25], [26]. However, these devices require a lot of maintenance and are extremely expensive, which limits their use to research and development purposes: it would be uneconomical to equip a whole potline with such devices.
The solution presented in this article is an alternative to these measuring devices. It is based on a photo-acoustic analyzer: a sample of pot gas is taken from the duct and passes into a chamber where a laser emitting at a carefully chosen frequency will selectively excite CF_4 molecules so that they emit a sound whose amplitude is directly related to the quantity of CF_4 present.

The gas analyzer, developed by Mirsense, is fully operational; further development has focused on the gas sampling system, in order to obtain a complete system with limited maintenance and low cost, suitable for applying to every pot in a smelter.

2. Principle of Photoacoustic Spectroscopy Technology

The photoacoustic effect was discovered in 1880 by Alexander Graham Bell [27]. This effect, illustrated in Figure 1, designates the generation of sound waves by a solid, liquid or gas illuminated by an electromagnetic wave modulated at an acoustic frequency. The absorption of the light radiation heats up the target material, and the radiation causes cycles of dilation and compression under that periodic heat load. The dilation and compression cycles constitute the source of the acoustic waves [28].

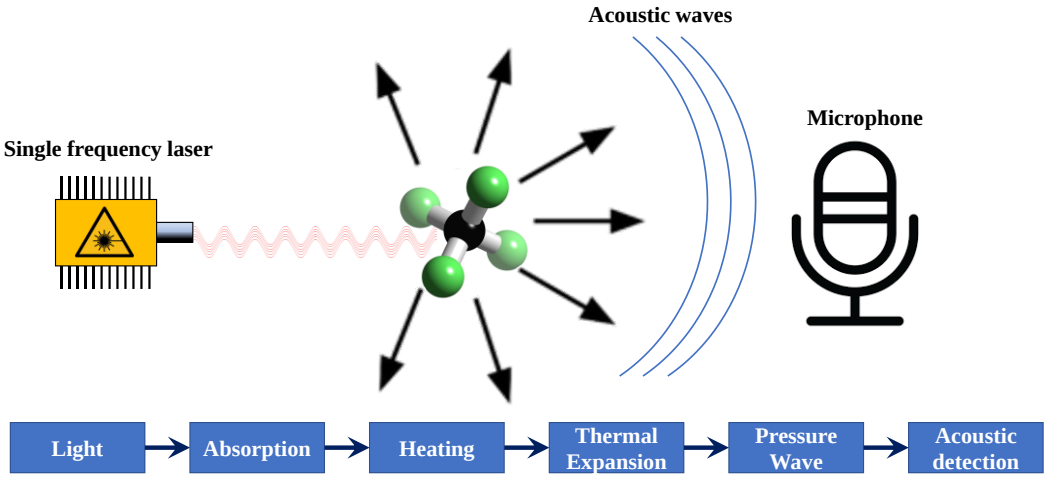

Figure 1. Principle of operation for laser photoacoustic spectroscopy.

The photoacoustic effect applied to gas is today one of the most sensitive laser spectroscopy techniques for local detection. Using a source of laser light whose wavelength matches the spectral fingerprint of the particular molecule to be identified, an acoustic signal results if the molecule is present in the sample under analysis.

An important technique for amplifying the acoustic signal consists in hosting the photoacoustic effect within a resonant gas cell. Gas cells are therefore geometrically designed to resonate at a specific frequency, increasing the sound pressure to a degree described by the resonance factor. This technique has several advantages [29]:

- First, it is remarkably sensitive: reducing the gas cell volume increases the pressure of the acoustic waves, making it possible to reduce the size of the sensor. The small cell volume (1 ml) requires only a very small flow rate, reducing the gas consumption for the measurement and thus the environmental impact of the exhaust gas.
- There is no zero drift: the photoacoustic technique is a background free technique, meaning that no signal is observed in the absence of the target molecule. This is a true advantage over numerous other techniques requiring a background signal reset. Problems due to drift are eliminated.
- The photo-acoustic sensors can be very compact and inexpensive (Micro Electro Mechanical Systems microphones).
- The technique has a large dynamic range with up to six decades of linearity, making it possible to detect concentrations from as low as a few ppb up to as high as several percent without recalibration. Microphones are also achromatic detectors: they do not depend on the wavelength of the targeted molecular fingerprint. This property simplifies the multi-gas sensors, which remain cost effective and compact, having no need of multiple detectors or sophisticated filters or coatings.
- Finally, the technique is very robust. The microphones do not use any optics, which is an outstanding advantage: no collimation optics and no mirrors are required in the set-up, avoiding mirror misalignment and contamination, making the sensor robust to external shocks and to pollution of the gas cell.

3. Photo-acoustic Detector for Aluminum Smelters

The measuring system is illustrated in Figure 2, and consists of the following elements:

- A system for sampling the pot gases in the collection duct,
- A dust filter and a trap to capture the fluorinated vapors,
- A photoacoustic spectrometer together with its signal processing electronics.

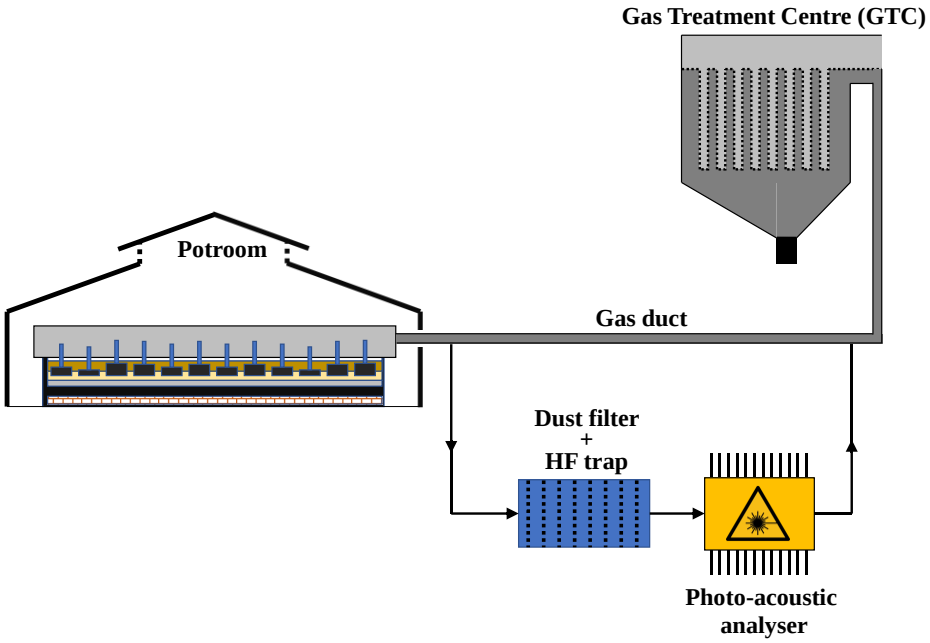

Figure 2. Schematic diagram of the gas sampling line.

The photo-acoustic measuring device shown in Figure 3 (Quantum Cascade Laser, gas chamber and microphone) requires a very small amount of gas to operate. To supply the measuring system, a very small hole was made in the collection duct at the pot outlet in which a pipe was installed. This pipe carries a sample of the pot gases through the dust filter and fluorinated vapors trap to the analysis chamber of the photoacoustic detector. After passing through the analyzer, the gas sample is returned to the collection duct a little further downstream. Our objective is to build such a device that can be installed on every single pot in a complete potline. The device must therefore be inexpensive and require minimum maintenance.

Figure 3. MultiSense gas analyser

4. Experimental Results

We tested our new gas analyzer on an APXe technology prototype pot at the Laboratoire de Recherche des Fabrications (LRF) of Rio Tinto Aluminium Pechiney, in Saint Jean de Maurienne. As the LRF pots are dedicated to R&D, they are equipped with numerous continuous measurements, unlike pots in industrial smelters. In particular, we have, for each of these pots, a Fourier Transform Infra-Red spectrometer (FTIR) which allows us to measure on-line the concentration of different gases at the outlet (CO, CO_2, CF_4, C_2F_6, etc.). We therefore placed our photo-acoustic spectrometer in parallel with the FTIR analyzer on one of these pots, in order to compare the performances of the two devices in measuring the CF_4 concentration.

Once the photoacoustic analyzer was installed on the pot, we waited for an anode effect to occur, in order to verify that it had been detected and to be able to compare the measurements obtained with those of the FTIR spectrometer. The first anode effect occurred on April 19, 2022 at about 17:17 h.

In Figure 4, the pot voltage is shown in green (left vertical scale). It can clearly be seen that this voltage remains stable at around 4 volts and then increases in just a few seconds at the time of the declaration of the anode effect, at around 17:17 h. When the voltage exceeds 8 volts, ALPSYS® - the pot process control system - automatically starts an anode effect treatment (which explains the observed fluctuations of the pot voltage) and the voltage quickly returns to a "normal" value, close to 4 volts. In the lower part of Figure 4 we see in blue the photo-acoustic analyzer measurement of the CF_4 content of the pot gases, and in orange this same measurement carried out by the FTIR spectrometer.

In both cases, there is a sudden increase in the CF_4 concentration at the time of the declaration of the anode effect (at 17:17 h) to reach a maximum concentration close to 500 ppm. A slight difference can be observed between the two curves. It can be explained by the fact that the FTIR analyzer performs only one measurement per minute while the photo-acoustic spectrometer makes two measurements per second. We can therefore draw as a first conclusion that the photo-acoustic analyzer is well able to detect the anode effect and that the concentration it measures is of the same order of magnitude as that of the FTIR analyzer, with a much faster response than the latter.

However, there is not much point in detecting the appearance of CF_4 when the anode effect has already been declared by the regulation system (i.e., when the pot voltage exceeds 8 volts). Much more interestingly, a notable increase in the rate of CF_4 is detected before the anode effect is visible in the pot voltage. In Figure 5, which shows the same data as Figure 4 but with a CF_4 concentration scale between 0 and 4 ppm, we observe from 16:58 h, an increase in the rate of CF_4, visible both with the FTIR analyzer and the photo-acoustic spectrometer. In this case, it was possible to detect the precursors of an anode effect 19 minutes before it occurred, leaving enough time to take action to avoid the effect.

CF_4 (and C_2F_6) appear in the pot gases as soon as the concentration of oxyfluoride ions under an anode is too low and leads to reaching the limiting current density. The anodic electrochemical half-reaction then switches to another system involving fluoride ions, present in large quantities in the bath, and the anodic carbon. A continuous CF_4 detector therefore makes it possible to detect the anode effects very early on. The advantage of the photoacoustic spectrometer (with the associated gas sampling, dust filtration and fluoride trapping equipment) is that the total cost for a complete potline is low enough to make the system economically advantageous. It is estimated that the cost per pot of the installed device will be a few thousand euros (whereas the cost of an FTIR analyzer is amounts to several tens of thousands euros).

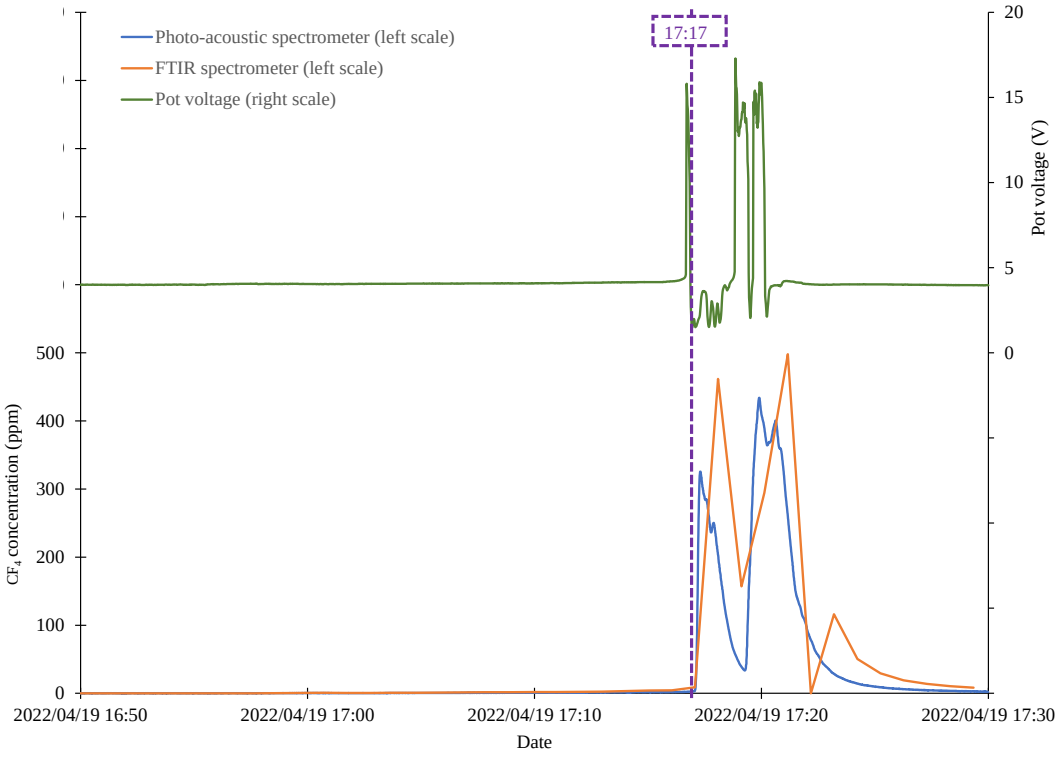

Figure 4. CF_4 concentration (0 - 500 ppm) and pot voltage during the anode effect.

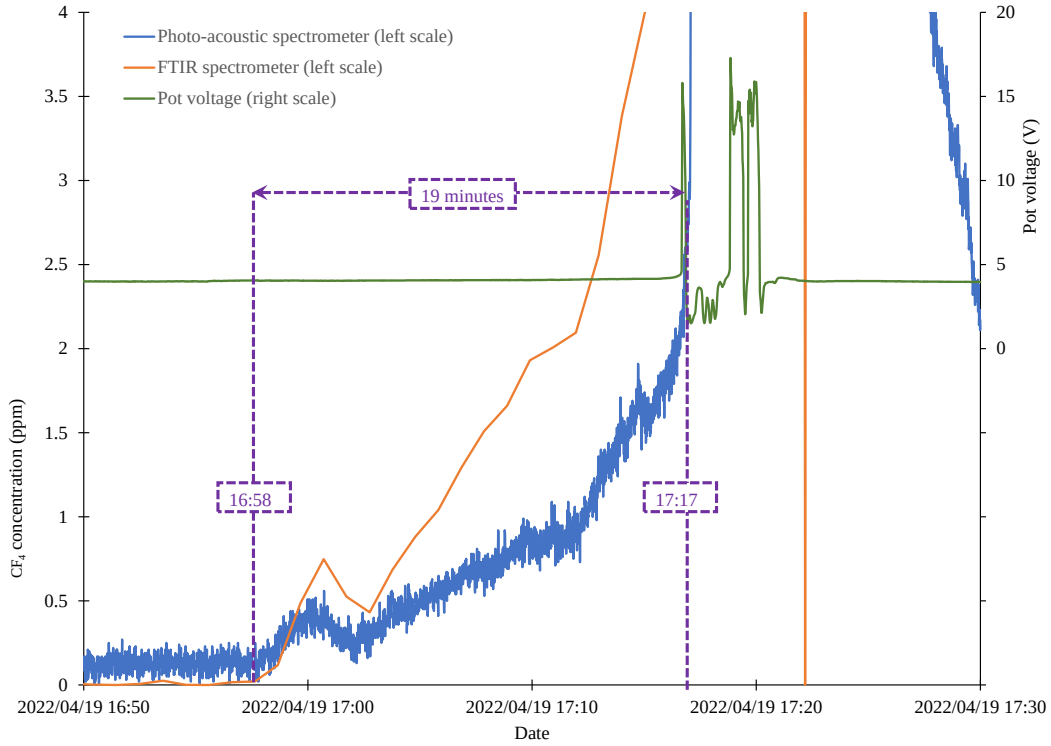

Figure 5. CF_4 concentration (0-4 ppm) and pot voltage during the anode effect.

5. Industrial Perspectives

We have now completely validated the operation of the MultiSense gas analyzer (QCL lasers, gas chamber and microphone) for detecting CF_4.

Regarding the sampling system (dust filtration and fluoride trapping), the objective is clearly to achieve a low-cost device with limited maintenance. To date, we have operated the device for more than a month without any intervention and we reasonably hope to reach six months of maintenance-free operation for the industrial system, when it will be generalized to all the pots in a complete line.

In parallel to the development of the system, we are working on making it entirely wireless, so that its installation is as simple and inexpensive as possible. We therefore intend to couple the system with a self-powered device (probably based on the temperature difference between the gas duct and the surrounding air, using the Seebeck effect) and to ensure that the measurement information from the sensor is sent wirelessly via an appropriate radio protocol.

Once this sensor has been developed and deployed on all the pots in a line, it will then be possible to develop, in the pot control system, an algorithm for the preventive treatment of anode effects which will be activated as soon as the CF_4 content exceeds a certain threshold. Contrary to anode effect prediction algorithms, which have a significant false positive rate, the appearance of CF_4 is caused by a real and proven lack of oxyfluoride ions, i.e., by a real lack of alumina in the pot. This will prevent any unnecessary launching of a preventive treatment of anode effect which would lead to depositing undissolved alumina on the cathode. The preventive treatment will also be less harmful to the cell than the standard anode effect treatment.

Finally, as mentioned at the beginning of this paper, several authors have shown that a significant part of the CF_4 produced by the pots is outside the declared anode effect. That is to say that this CF_4 is released during the long minutes before the moment when the cell voltage has taken off, but CF_4 is nevertheless forming under one or more anodes because of a too low local concentration of oxyfluoride ions. Thus, the MultiSense gas analyzer would be a good way to express the amount of CO_2 equivalent released per ton of aluminum produced taking into account not only the actual CO_2 but also the PFCs, and hence know the real impact of a pot on global warming.

6. Conclusions

Applying the MultiSense gas analyzer to all the pots in a line will make it possible to drastically reduce the frequency of anode effects and thus not only improve the performance of the pots but also significantly reduce their damaging effect on the environment.

This continuous measurement of CF_4 also opens up new perspectives in the regulation of the alumina content of the pots. To date, the algorithm is based on an alternation between over and underfeeding because there is no industrially available continuous sensor of the alumina content of the pots. With a measurement of the CF_4 concentration of the pot gases, it would be possible to operate the alumina feeders at a constant rate, estimated according to the amperage of the cell and its assumed current efficiency. This rate would be very slightly shortened over time until the appearance of CF_4 in the pot gases, this phenomenon being the indicator of the achievement of the minimum alumina content in the bath. It would thus be possible to regulate the alumina content of the pots with very small variations in the feeding periods and thus tighten the resistance of the pots around the set value, which would significantly improve their performance.

7. References

1. Jomar Thonstad, Pavel Fellner, Geir Martin Haarberg, Ján. Híveš, Halvor Kvande and Åsmund Sterten, *Aluminium Electrolysis — Fundamentals of the Hall-Héroult Process,* 3rd Edition, Aluminium-Verlag, 2001, 359 pages.
2. Alton T. Tabereaux, Anode effects, PFCs, global warming, and the aluminum industry, *Journal of the Minerals, Metals and Materials Society*, Vol. 46, No. 11 (1994), 30-34.
3. Helmut Vogt, Contribution to the interpretation of the anode effect, *Electrochimica Acta*, Vol. 42 , No. 17 (1997), 2695-2705.
4. Helmut Vogt, Effect of alumina concentration on the incipience of the anode effect in aluminium electrolysis, *Journal of Applied Electrochemistry*, Vol. 29 (1999), 779-788.
5. Helmut Vogt and Jomar Thonstad, Review of the causes of anode effects in aluminium electrolysis, *Aluminium*, Vol. 79, No. 1-2 (2003), 98-102.
6. Jomar Thonstad, F. Nordmo et K. Vee, On the anode effect in cryolite-alumina melts - I *Electrochimica Acta*, Vol. 18, No. 1 (1973), 27-32.
7. Jomar Thonstad, F. Nordmo and J. K. Rødseth, On the anode effect in cryolite-alumina melts - II The initiation of the anode effect, *Electrochimica Acta*, Vol. 19, No. 11 (1974), 761-769.
8. F. Nordmo et J. Thonstad, On the anode effect in cryolite-alumina melts – III Current voltage behaviour during anode effect, *Electrochimica Acta*, Vol. 29, No. 9 (1984), 1257-1262.
9. F. Nordmo et J. Thonstad, On the anode effect in cryolite-alumina melts - IV Gas composition and faradic efficiency, *Electrochimica Acta*, Vol. 30, No 6) (1985), 741-745.
10. Helmut Vogt and Jomar Thonstad, The voltage of alumina reduction cells prior to the anode effect, *Journal of Applied Electrochemistry*, Vol. 32, No. 3 (2002), 241–249.
11. Lukas Dion, Charles-Luc Lagacé, Laszlo Kiss and Sandor Poncsak, Using Artificial Neural Network to Predict Low Voltage Anode Effect PFCs at the Duct End of an Electrolysis Cell, *Light Metals* 2016, 545-550.
12. C. Cheung, C. Menictas, J. Bao, M. Skyllas-Kazacos and B. J. Welch, Frequency response analysis of anode current signals as a diagnostic aid for detecting approaching anode effects in aluminium smelting cells, *Light Metals* 2013, 887-892.
13. Nazatul Aini Abd Majid, Mark P. Taylor, John J. J. Chen and Brent R. Young, Multivariate statistical monitoring of the aluminium smelting process, *Computers and Chemical Engineering*, Vol. 35 (2011), 2457- 2468.
14. N. Aini Abd Majid, M. P. Taylor, J. J. J. Chen, M. A. Stam, A. Mulder and B. R. Young, Aluminium process fault detection by Multiway Principal Component Analysis, *Control Engineering Practice*, Vol. 19 (2011), 367-379.
15. Lucas José da Silva Moreira, Gildas Besancon, Francesco Ferrante, Mirko Fiacchini and Hervé Roustan, Model Based Approach for Online Monitoring of Aluminium Production Process, *Light Metals* 2020, 566-571.
16. Lucas José da Silva Moreira, Mirko Fiacchini, Gildas Besançon, Francesco Ferrante and Hervé Roustan, Modeling and observer design for aluminum manufacturing, *European Journal of Control*, Vol. 64 (2022), 100611.
17. Ron Kremser, Niclas Grabowski, Roman Düssel, Albert Mulder and Dietmar Tutsch, Anode Effect Prediction in Hall-Héroult Cells Using Time Series Characteristics, *Applied Science*, Vol. 10 (2020), 9050.
18. Abdelhamid Meghlaoui, Jules Thibault, R. T. T. Bui, Laszlo Tikasz and Renaud Santerre, Neural networks for the identification of the aluminium electrolysis process, *Computers & Chemical Engineering*, Vol. 22, No. 10 (1998), 1419-1428.
19. K. Zhou, D. Yu, Z. Lin, B. Cao, Z. Wang and S. Guo, Anode effect prediction of aluminum electrolysis using GRNN, *Chinese Automation Congress (CAC)*, Wuhan, China, 2015.

20. A. Johnson et L. Ching-Chung, Wavelet Packet Timeseries Analysis of Aluminum Electrolytic Cells, *Proceedings of The International Society for Optical Engineering*, Vol. 4391 (2001), 228-237.
21. Y. Zhang, Study on Anode Effect Prediction of Aluminium Reduction Applying Wavelet Packet Transform, *Advanced Intelligent Computing Theories and Applications*, (2010), 477-484.
22. W. Haupin, E. J. Seger, Aiming for Zero Anode Effects, *Essential Readings in Light Metals: Volume 2, Aluminum Reduction Technology, Springer International Publishing*, Berlin/Heidelberg, Germany, 2016, 767-773.
23. Thor A. Aarhaug, Alain Ferber, Heiko Gaertner, Steinar Kolås, Sven Olof Ryman, and Peter Geiser, Validation of Online Monitoring of PFC by QCL with FTIR Spectroscopy, , *Light Metals* 2018, 1487-1493.
24. Jomar Thonstad and Sverre Rolseth, Low Voltage PFC Emission from Aluminium Cells, *Journal of Siberian Federal University - Chemistry*, Vol. 10, No. 1 (2017), 30-36.
25. Wangxing Li, Qingyun Zhao, Jianhong Yang, Shilin Qiu and Xiping Chen, On Continuous PFC Emission Unrelated to Anode Effects, *Light Metals* 2011, 309-314.
26. David S. Wong, Paul Fraser, Pascal Lavoie, and Jooil Kim, PFC Emissions from Detected Versus Nondetected Anode Effects in the Aluminum Industry, *Journal of the Minerals, Metals and Materials Society*, Vol. 67, No. 2 (2015), 342-353.
27. Alexander Graham Bell, On the Production and Reproduction of Sound by Light, *American. Journal of Science*, Vol. 20 (1880), 305-324.
28. Stefan Palzer, Photoacoustic-Based Gas Sensing: A Review, *Sensors*, Vol. 20 (2020), 2745.
29. Mirsense OEM gas analyser, https://mirsense.com/liste-produits/371-2/